

available at www.sciencedirect.comjournal homepage: www.elsevier.com/locate/ijrefrig

Application of waste heat powered absorption refrigeration system to the LNG recovery process

Paul Kalinowski^a, Yunho Hwang^{a,*}, Reinhard Radermacher^a, Saleh Al Hashimi^b, Peter Rodgers^b

^aCenter for Environmental Energy Engineering, Department of Mechanical Engineering, University of Maryland, College Park, MD 20742, USA

^bThe Petroleum Institute, Abu Dhabi, United Arab Emirates

ARTICLE INFO

Article history:

Received 30 October 2008

Received in revised form

16 January 2009

Accepted 21 January 2009

Published online 4 February 2009

Keywords:

LNG

Liquefaction

Vapour

Absorption system

Ammonia-water

Heat recovery

Cogeneration

Gas turbine

ABSTRACT

The recovery process of the liquefied natural gas requires low temperature cooling, which is typically provided by the vapor compression refrigeration systems. The usage of an absorption refrigeration system powered by waste heat from the electric power generating gas turbine could provide the necessary cooling at reduced overall energy consumption. In this study, a potential replacement of propane chillers with absorption refrigeration systems was theoretically analyzed. From the analysis, it was found that recovering waste heat from a 9 megawatts (MW) electricity generation process could provide 5.2 MW waste heat produced additional cooling to the LNG plant and save 1.9 MW of electricity consumption. Application of the integrated cooling, heating, and power is an excellent energy saving option for the oil and gas industry.

© 2009 Elsevier Ltd and IIR. All rights reserved.

Système frigorifique à absorption entraîné par la chaleur récupérée : application dans le processus de récupération du GNL

Mots clés : GNL ; Liquéfaction ; Vapeur ; Système à absorption ; Ammoniac-eau ; Récupération de chaleur ; Cogénération ; Turbine à gaz

* Corresponding author. Tel.: +1 301 405 5247; fax: +1 301 40 2025.

E-mail address: yhhwang@umd.edu (Y. Hwang).

0140-7007/\$ – see front matter © 2009 Elsevier Ltd and IIR. All rights reserved.

doi:10.1016/j.ijrefrig.2009.01.029

Nomenclature

| | |
|-------|----------------------------------|
| ARS | absorption refrigeration system |
| CHP | cooling, heating and power |
| COP | coefficient of performance |
| COND | condenser |
| FLASH | flash drum |
| GEN | generator |
| GUI | graphical user interface |
| IPA | intermediate pressure evaporator |

| | |
|------|----------------------------------|
| IPE | intermediate pressure evaporator |
| kW | kilowatts |
| LNG | liquefied natural gas |
| LPA | low pressure absorber |
| LPE | low pressure evaporator |
| MW | megawatts |
| RECT | rectifier |
| SHX | solution heat exchanger |

1. Introduction

Oil and gas industry consumes a large amount of thermal energy in the form of heat or steam for various chemical processes as well as mechanical and/or electrical energy to drive compressors and pumps. In the oil and gas industry, gas turbines are typically used to drive mechanical equipment and to generate electricity. When gas turbines are used for power generation on-site, they are well suited for the combined cooling, heating and power (CHP) powered by the high temperature waste heat, which is normally discharged to the surroundings.

Furthermore, CHP technologies can be coupled with existing and planned technologies in the industrial, commercial, and residential sectors. CHP involves on-site or near-site generation of electricity along with utilization of thermal energy available from the power generation process. Popovic et al. (2002) utilized the waste heat from the power generating microturbine to drive an absorption chiller and subsequently to regenerate a solid desiccant system for cooling the educational building. They reported that they achieved total energy utilization was 78% from conversion of natural gas. Hwang (2004) extended the same CHP concept by proposing the cooling capacity provided from the absorption chiller to be utilized either to subcool the liquid exiting the condenser of the refrigeration system, to precool the air entering the condenser in the refrigeration system, or to precool the microturbine intake air. He claimed that this approach enhances the part load microturbine efficiency and the proposed CHP system could reduce the annual energy consumption up to 19% as compared to a refrigeration system operating without any waste heat utilization from the microturbine. Nayak et al. (2009) characterized the performance of the gas engine generator integrated with a liquid desiccant dehumidification system and reported that the CHP efficiency ranged from 66% to 75%. Kong et al. (2004) proposed the CHP system with an available Stirling engine and claimed that such CHP system could save more than 33% of the primary energy compared to a conventional independent system. Wu and Wang (2006) provided a review on combined CHP systems. They provided overview of the definition and benefits of CHP systems, the characteristics of CHP technical performances, diverse CHP configurations of existing technologies, and the worldwide status of CHP development. Wu and Wang concluded that promising CHP technologies could grow with the cooperative efforts of governments, energy-

related enterprises and professional associations within decades. The recovered waste heat can then be utilized for heating in chemical processes or converted to the cooling for powering absorption refrigeration systems (ARS). For example, a waste heat powered ammonia–water ARS was installed at the Ultramar Diamond Shamrock refinery to recover propane and higher molecular weight hydrocarbons that were flared continuously (Brant et al., 1998; Erickson, 2000; Erickson et al., 1998). The ARS was powered by low temperature (143 °C) heat source from the reformer and enables to cool the gas to –31.7 °C, thereby recovering 45% of high molecular weight hydrocarbons. In addition, the ARS allowed cooling of the wet gas vapor to 4.5 °C at the compressor inlet and enhanced the performance of the fluidized catalyst cracker. Although there are a lot of potential applications of a CHP in the oil and gas industry, it has not been extensively explored yet. In this study, a liquefied natural gas (LNG) plant process is analyzed as a potential application of a CHP to achieve more energy efficient LNG production.

2. Modeling of LNG plant process

2.1. Current LNG plant process

During the LNG production process, the high molecular weight hydrocarbons are extracted from the associated gas, liquefied, dehydrated, and finally sent to a fractionation plant. Two propane vapor compression chillers are used to cool the associated gas to 18 °C in the first chiller and to –42 °C in the second chiller (Fig. 1a). Both chillers use electrical energy provided by a gas turbine.

2.2. LNG plant with heat recovery

High temperature exhaust gas from the gas turbine is discharged to the surroundings. Potentially, it could be used to power an ARS, which would replace the propane vapor compression refrigeration systems by providing the necessary cooling for the associated gas. The ARS would save energy consumption of the LNG plant and reduce emissions from it. Fig. 1b illustrates the schematic of the integrated ARS as a replacement of the refrigeration system.

This paper reports details of the analysis undertaken to determine the cooling capacity of the refrigeration system,

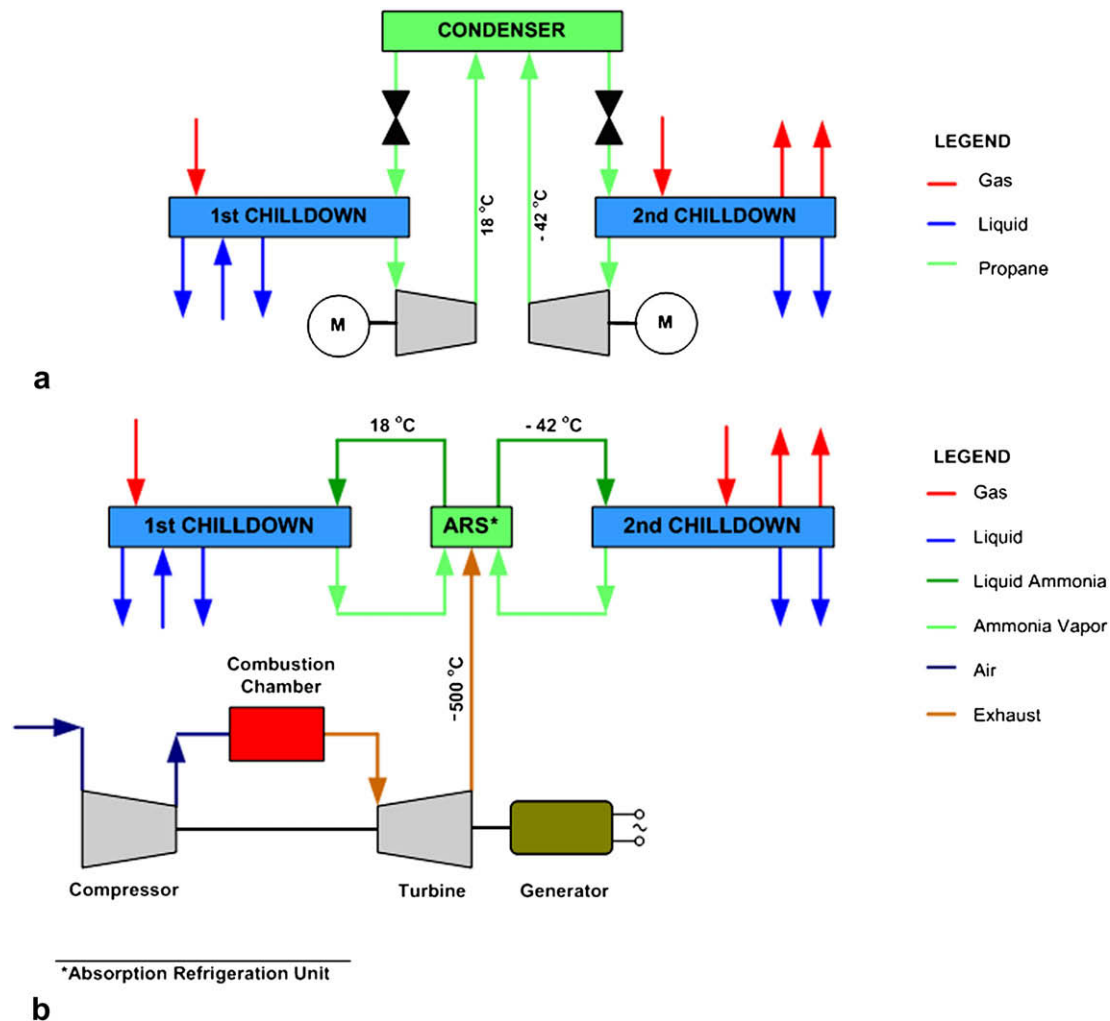


Fig. 1 – Schematics of LNG processes with (a) propane refrigeration systems and (b) absorption refrigeration systems.

minimum amount of waste heat from the gas turbine which can be utilized to power the ARS, and the ARS baseline. For the analysis, vapor compression cycle, gas turbine per generation cycle, and absorption cycle were modeled using the Engineering Equation Solver (F-chart Software, 2008) as a modeling platform. In the modeling, several parameters were considered from an LNG plant operating in the Persian Gulf with a 560 m³ of hourly LNG production capacity.

2.3. Propane chiller modeling

The propane chillers were modeled to determine the cooling capacity required for the LNG plant process. The following assumptions were made for the chiller models:

- No pressure drops through the evaporator, condenser, and connecting pipes.
- Negligible kinetic and potential energy.
- Constant refrigerant flow rate.
- Saturated vapor at the compressor inlet.
- Saturated liquid at the condenser exit.
- Compressor power input, 1000 kilowatts (kW).

- Isentropic compressor efficiency, 60%.
- Heat rejection temperature at the condenser exit, 50 °C.
- Evaporating temperature, 18 °C and -42 °C for first and second chiller, respectively.

Table 1 summarizes the modeling results of both chillers. At the same compressor work, the refrigerant flow rate of the first chiller is approximately four times higher than that of the second chiller because of the higher density at the suction, and accordingly higher specific work of the compressor. Both the refrigeration capacity and the coefficient of performance (COP) of the first chiller are approximately five times higher than those of the second chiller.

2.4. Gas turbine modeling

A simple gas turbine power generation cycle essentially consists of a compressor, a combustion chamber, and a turbine. To simplify the complexity of the process in the open cycle gas turbines, an idealized air-standard analysis is applied to study their performance. The Brayton cycle is an air-standard cycle used to analyze the gas turbine process.

Table 1 – Modeling results for the chillers.

| Chiller | First chiller | Second chiller |
|------------------------------|---------------|----------------|
| Propane flow rate (kg/s) | 16.89 | 4.47 |
| Evaporating temperature (°C) | 18 | –42 |
| Cooling capacity (kW) | 4,329 | 842 |
| Compressor power (kW) | 1,000 | 1,000 |
| COP (–) | 4.33 | 0.84 |

The following assumptions were used in the air-standard analysis (Moran and Shapiro, 2004):

- Air is the working fluid, which behaves as an idea gas.
- The combustion is replaced by a heat addition at constant pressure.
- The exhaust of combustion products is replaced by a heat rejection at constant pressure.

The gas turbine model was developed by applying generic off-design characteristics. Specifications of the gas turbine selected in this study are summarized in Table 2 (Erickson et al., 1998). The gas turbine generates approximately 9 megawatts (MW) at the ISO conditions. Since it was assumed that the mass flow rate through the compressor was the same as that through the turbine, the exhaust flow rate was assumed to be the air mass flow rate for modeling purpose. The isentropic efficiencies of the compressor and turbine were assumed to be 83% and 84.5%, respectively. The gearbox and generator efficiency were assumed to be 99% and 97%, respectively. All other pressure and mechanical losses were neglected. The graphical user interface (GUI) of the gas turbine model is illustrated in Fig. 2. First, manufacturer's data (mass flow rate, pressure ratio, and exhaust temperature), operating

Table 2 – Gas turbine specifications.

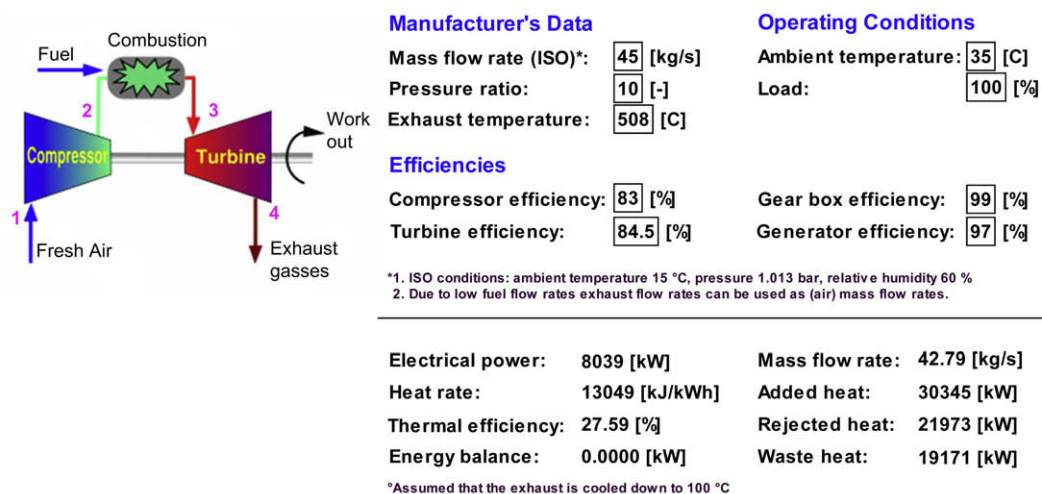
| | |
|--|------|
| Pressure ratio (–) | 10 |
| Turbine inlet temperature (°C) | 975 |
| Exhaust gas temperature (°C) | 508 |
| Exhaust gas flow rate (kg/s) | 45 |
| Electrical power output at ISO condition ^a (kW) | 8963 |
| Thermal efficiency (–) | 0.27 |
| Shaft speed (RPM) | 8000 |

^a The ISO conditions are: 101.3 kPa ambient pressure; 15 °C ambient temperature; and 60% relative humidity.

conditions (ambient temperature and load ratio), and efficiencies of compressor, turbine, gearbox, and generator are set. Then output parameters of the gas turbine such as electrical power output, thermal efficiency, amount of heats, mass flow rate and thermodynamic properties of fluids are determined. Table 3 summarizes the major results of the gas turbine model. Compressor discharge pressure and turbine inlet temperature are 101.3 kPa and 976.5 °C, respectively. Due to compression losses compressor discharge temperature is higher than it would be at the isentropic compression. The high turbine exit temperature is attributed to expansion losses in the turbine. The modeled thermal efficiency of the Brayton cycle is 0.29, which is typical for gas turbines of this size. Approximately 71% of added energy to the gas turbine, 23 MW, is “wasted” by rejecting it to surroundings. A portion of this heat, 19 MW, could be utilized to power an ARS by cooling it to 100 °C.

2.5. Absorption refrigeration system modeling

Since the LNG process requires subfreezing temperature refrigeration for its LNG recovery process, an ammonia–water



| | T [C] | p [bar] | h [kJ/kg] | s [kJ/kg-K] |
|---|-------|---------|-----------|-------------|
| 1 | 35 | 1.013 | 308.6 | 5.729 |
| 2 | 365.2 | 9.69 | 647.8 | 5.826 |
| 3 | 993.8 | 9.69 | 1357 | 6.594 |
| 4 | 526.7 | 1.013 | 822.1 | 6.717 |

Fig. 2 – The GUI of the gas turbine model.

Table 3 – Modeling results for the gas turbine at ISO conditions.

| | |
|------------------------------|--------|
| Thermal efficiency (–) | 0.29 |
| Electrical power output (kW) | 9,038 |
| Mass flow rate (kg/s) | 45 |
| Added heat (kW) | 32,399 |
| Rejected heat (kW) | 23,087 |
| Waste heat (kW) | 19,236 |

pair is selected instead of a water–lithium bromide pair as its working fluids. The ammonia–water absorption machines are primarily designed for industrial refrigeration applications with evaporating temperatures as low as -60°C (EU Commission, 2001). Therefore, it covers all evaporating temperatures of interest in the current study. Furthermore, more compact size of the first system than the second would facilitate an easy integration into the process.

Two single-effect and one double-lift ammonia–water absorption refrigeration cycles were modeled to analyze their potential application to the LNG process. The following assumptions were made for the models:

- Only the waste heat from the gas turbine powers the absorption cycles.
- No pressure changes except through the expansion valves and pumps.
- Heat losses to the surroundings are negligible.
- Saturated liquid at the exit of the condensers, absorbers, and generators.
- Saturated vapor at the rectifier outlet with 0.99 ammonia concentration.
- Isentropic pump efficiency 85%.
- Heat exchanger efficiency 80%.
- Heat rejection temperature at the condenser and absorber outlet 50°C .
- Saturated vapor temperature at the evaporator outlet 18°C and -42°C for first and second chiller, respectively.

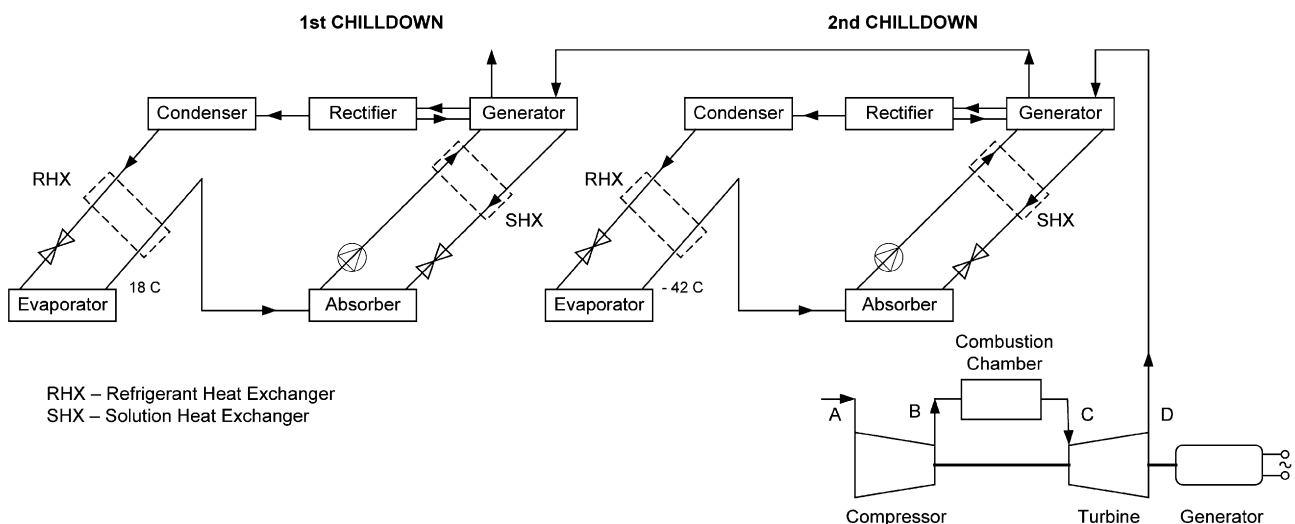
Table 4 – Modeling results for the single-effect absorption refrigeration system.

| Chiller | First | Second |
|---|-------|--------|
| Heat transfer rate in generator (kW) | 7606 | 4841 |
| Exhaust temperature at generator inlet ($^{\circ}\text{C}$) | 348 | 453 |
| Exhaust temperature at generator exit ($^{\circ}\text{C}$) | 177 | 348 |
| Pump work (kW) | 21.28 | 37.16 |
| Maximum pressure (kPa) | 2015 | 2015 |
| COP (–) | 0.57 | 0.17 |
| Total system COP (–) | 0.41 | |

The gas turbine was assumed to operate at 35°C ambient temperature and 80% load. The calculated exhaust mass flow rate and temperature were 42.86 kg/s and 453.4°C , respectively. Thermodynamic properties of ammonia–water solution developed by Ibrahim and Klein (1993) were used for absorption refrigeration modeling.

2.6. Single-effect ammonia–water ARSs

Fig. 3 shows the ammonia–water ARS consisted of two single-effect absorption systems. One of the systems could replace the first chiller while the other system could replace the second chiller. The exhaust gas of the gas turbine powers the generator of the second chiller, and then the cooler exhaust powers the generator of the first chiller. Solution and refrigerant heat exchangers are employed to increase the performance of the systems. The rectifiers are also used to increase the performance of the system by increasing the ammonia concentration in the ammonia–water vapor mixture. The cooling loads for the evaporators were taken from the propane chiller models. The generator (maximum) temperature was set to be 190°C . Table 4 summarizes the major results of the ARS consisted of two single-effect ARSs. Higher cooling load of the first chiller requires higher refrigerant flow rate, consequently higher generator heat transfer rate, and higher exhaust temperature glide than those of the second chiller.

**Fig. 3 – Schematic of the single-effect ammonia–water absorption refrigeration system.**

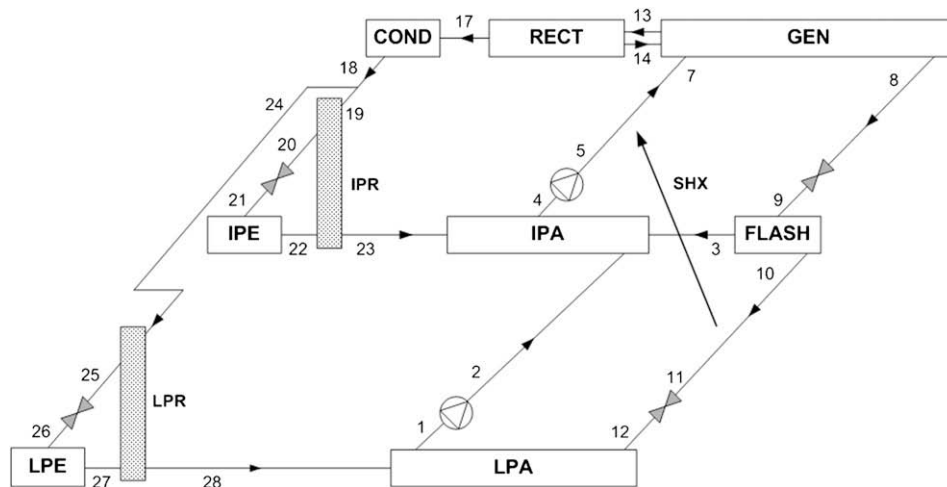


Fig. 4 – Schematic of the double-lift ammonia-water absorption refrigeration system.

The ammonia concentration, vapor quality, and heat rejection temperature in the condenser determine the maximum pressure which is 2015 kPa in both systems. The low COP of the second ARS is due to high heat transfer rate in the generator and high pump work to achieve low evaporating temperature. In overall, two ARSs require over 12 MW exhaust heat to power the generators. Total COP of the ARS is approximately 0.41.

2.7. Double-lift ammonia-water ARS

Fig. 4 illustrates a double-lift ammonia-water ARS. This cycle has two evaporator pressure levels with a low pressure absorber (LPA) serving for the low pressure evaporator (LPE), and an intermediate pressure absorber (IPA) serving for the

intermediate pressure evaporator (IPE). The refrigerant vapor is generated from the weak solution in the generator (GEN) and rectified in the rectifier (RECT) to increase the ammonia concentration. After the condensation process in the condenser (COND), the liquid refrigerant is split into two streams for the IPE and the LPE. The flash drum (FLASH) is applied to lower the generator temperature. Steam generated by decreasing pressure is separated in the FLASH and flows into the IPA to increase its temperature. The liquid solution flows into the LPA. The intermediate pressure refrigerant heat exchanger (IPR), low pressure refrigerant heat exchanger (LPR), and the solution heat exchanger (SHX) are employed to increase the efficiency of the cycle. The rectifier (RECT) is used to increase the ammonia concentration and thus the performance of the system. The IPE and LPE could replace the first

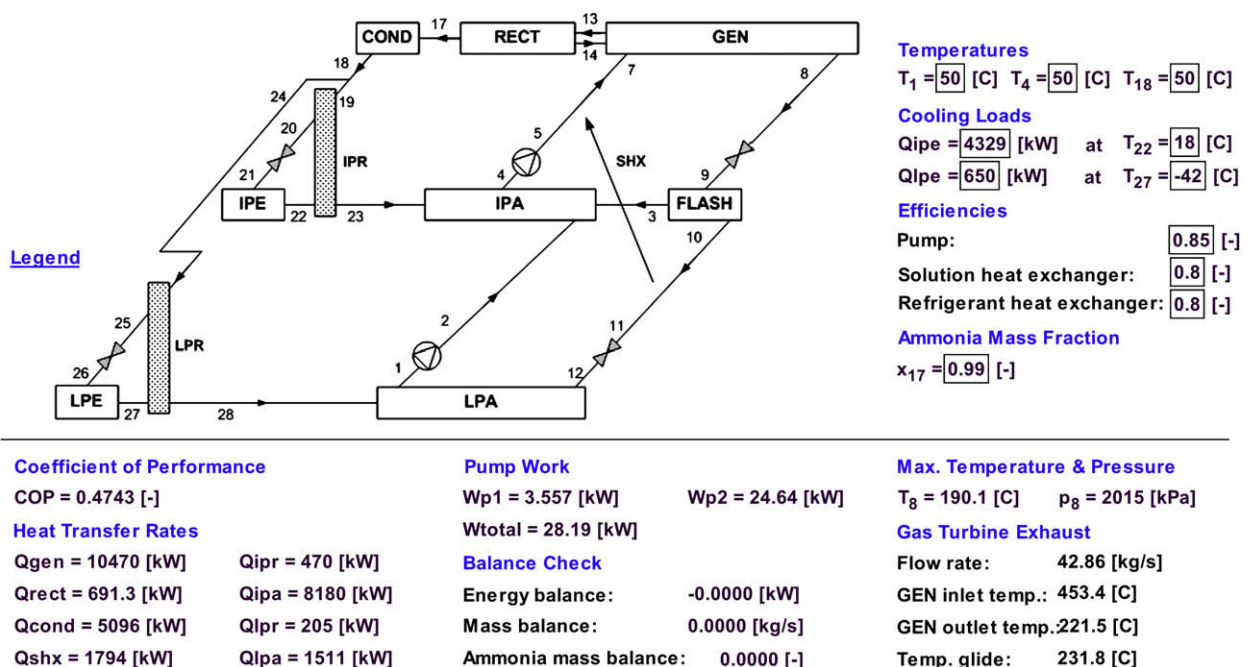


Fig. 5 – The GUI of the double-lift absorption refrigeration system model.

Table 5 – Modeling results for the double-effect absorption refrigeration system.

| | |
|---|--------|
| Heat transfer rate in generator (kW) | 10,470 |
| Exhaust temperature at generator inlet (°C) | 453.4 |
| Exhaust temperature at generator exit (°C) | 222 |
| Total pump work (kW) | 28.19 |
| Maximum pressure (kPa) | 2,015 |
| Total system COP (–) | 0.47 |

chiller and the second chiller, respectively. The cooling loads of the evaporators and evaporating temperatures directly affect the generator temperature. Therefore, the cooling loads were adjusted in the ARS to keep the generator temperature low and consequently to reduce the additional water evaporation. The cooling load of the IPE was taken from the propane chiller model. However, the cooling load of the LPE was reduced from 842 kW to 650 kW due to too high generator temperature (above 200 °C). A GUI for the double-lift ARS was created as shown in Fig. 5. The interface contains fields for input variables which allow the user to change major parameters of the system. Besides, it also has fields for output variables to display major results. Furthermore, the link button to the gas turbine model facilitates the user to open the gas turbine computer model. The major results for the double-lift ammonia–water ARU are summarized in Table 5. The ARS requires over 10 MW exhaust heat to power the generator while the generator temperature reaches 190 °C. The exhaust gas from the gas turbine would be cooled by 232 K. Nearly 87% of the total pump work is performed by the solution pump, which delivers the solution from the IPA to the GEN. The maximum pressure, determined by the ammonia concentration, vapor quality, and heat rejection temperature in the condenser, increases to 2015 kPa. Total COP of the ARS is approximately 0.47.

3. Results

The results of two single-effect ammonia–water ARSs show that they could provide the required cooling load and completely replace the propane chillers. Although the double-lift ammonia–water ARS has fewer components, it could provide enough cooling load only for the first chiller and partly for the second chiller. Therefore, the single-effect ammonia–water ARS is more appropriate to replace the propane chillers used in the LNG plant. This option will contribute to the reduction of 1.9 MW electricity used to operate the vapor compression cycles in the conventional LNG plant. Hence, application of the integrated cooling and power is an excellent energy saving option for the oil and gas industry.

To investigate the effect of two evaporating temperatures used on the modeling results, the sensitivity analysis was conducted for the baseline propane cycle and the CHP system with single-effect ammonia–water ARS. Results for the high temperature evaporating temperature show that the size of the gas turbine and the electricity reduction by applying the CHP decrease by 0.5% and 2%, respectively, per a degree of evaporating temperature increase. Whereas, for the low temperature evaporating temperature show that the size of

the gas turbine and the electricity reduction by applying the CHP decrease by 2% and 1%, respectively, per a degree of evaporating temperature increase. These results are due to the increased cycle COP as the evaporating temperature increases. Different sensitivity of two evaporating temperatures is due to the absorption system being more sensitive to the low evaporating temperature than the vapor compression system does.

4. Conclusions

Most of the energy used for the electricity production and transportation is produced by burning fossil fuels such as coal, oil, and natural gas. Increasing cost of fossil fuels and concerns on climate changes spark public's interests in combined cooling, heating and power (CHP) technologies which simultaneously provide electrical power, heat, and cooling from a single energy source. CHP technologies increase the overall energy conversion efficiency and consequently reduce emissions. In this study, a LNG plant process was analyzed as a potential application of a CHP to achieve more energy efficient LNG production. To investigate the potential replacement of current propane chillers in the LNG plant with ARSs, the ARSs powered by waste heat from the power generating gas turbine was modeled. The modeling results demonstrate that the single-effect ammonia–water ARS could provide the required cooling load and completely replace the propane chillers, while the double-lift ammonia–water ARS could provide enough cooling loads only for the first chiller and partly for the second chiller. Providing 5.2 MW of waste heat produced additional cooling to the LNG plant by recovering the waste heat from a 9 MW electricity generation process could save 1.9 MW of electricity consumption. This means that application of the CHP to the oil and gas industry is worth for further investigation.

REFERENCES

- Brant, B., Brueske, S., Erickson, D.C., Papar, R., 1998. New waste-heat refrigeration system cuts flaring, reduces pollution. *Oil & Gas Journal*. May 18, 61–64.
- Erickson, D.C., 2000. LPG recovery from reformer treat gas. US Patent 6,158,241.
- Erickson, D.C., Anand, G., Papar, R.A., Tang, J., 1998. Refinery waste heat powered absorption refrigeration – cycle specification and design. *Proceeding of the ASME Advanced Energy System Division*. AES 38, 391–402.
- European Commission, Directorate General for Energy, 2001. SAVE II Programme: Energy Savings By CHCP Plants In The Hotel Sector, p. 10.
- F-Chart Software, 2008. Engineering Equation Solver. Madison, WI.
- Hwang, Y., 2004. Potential energy benefits of integrated refrigeration system with microturbine and absorption chiller. *Int. J. Refrigeration* 27 (8), 816–829.
- Ibrahim, O.M., Klein, S.A., 1993. Thermodynamic properties of ammonia–water mixtures. *ASHRAE Transactions*. Symposia 21 (2), 1495.
- Kong, X.Q., Wang, R.Z., Huang, X.H., 2004. Energy efficiency and economic feasibility of CCHP driven by stirling engine. *Energy Conversion and Management* 45 (9–10), 1433–1442.

- Moran, M., Shapiro, H., 2004. *Fundamentals of Engineering Thermodynamics*, fifth ed. John Wiley & Sons, New York, NY.
- Nayak, S.M., Hwang, Y., Radermacher, R., 2009. Performance characterization of gas engine generator integrated with a liquid desiccant dehumidification system. *Applied Thermal Engineering* 29, 479–490.
- Popovic, P., Marantan, A., Radermacher, R., Garland, P., 2002. Integration of Microturbine with single-effect exhaust-driven absorption chiller and solid wheel desiccant system. *ASHRAE Transactions* 108(2), HI-02-5-3.
- Wu, D.W., Wang, R.Z., 2006. Combined cooling, heating and power: a review. *Progress in Energy and Combustion Science* 32 (5–6), 459–495.